Chemical Engineering Journal 145 (2008) 25–31

Contents lists available at ScienceDirect

Chemical Engineering Journal

journal homepage: www.elsevier.com/locate/cej

Study on the carbon deposition in steam reforming of ethanol over Co/CeO_2 catalyst

H. Wang[a,b], Y. Liu[a,*], L. Wang[a], Y.N. Qin[a]

[a] Tianjin Key Laboratory of Applied Catalysis Science and Engineering, Department of Catalysis Science and Technology, School of Chemical Engineering, Tianjin University, Tianjin 300072, China
[b] School of Chemical Engineering, Inner Mongolia University of Technology, Huhehaot 010062, PR China

ARTICLE INFO

Article history:
Received 7 June 2007
Received in revised form 18 February 2008
Accepted 26 February 2008

Keywords:
Ethanol
Steam reforming
Carbon deposition
Coke
Cobalt
Ceria
Hydrogen

ABSTRACT

In this work, coke formation over Co/CeO_2 catalysts for the steam reforming of ethanol was studied. Variations of ethanol conversion and product distribution with reaction temperature and time were investigated and the used catalysts were characterized with thermal analysis method and transmission electron microscopy. The results indicate that the reaction temperature exerts influences on coke formation and its property significantly. As the reaction temperature is 450 °C or lower, catalyst particles are heavily enclosed by cokes, leading to severe deactivation. As the reaction temperature is 500 °C or 550 °C, the encapsulation of catalyst particles is rarely observed due to the formation of another kind of carbon, namely, tube- or fiber-like carbon, which results in mild deactivation. When the reaction temperature is over 600 °C, carbon deposition is not a major problem for the steam reforming of ethanol over Co/CeO_2 catalysts, for carbon deposition or coke formation under these temperatures is not notable.

1. Introduction

Hydrogen as an energy carrier has been attracting great attentions for the applications in power vehicles or small stationary power units [1]. Ethanol is an attractive option for the production of hydrogen since it is less toxic and can be produced renewably from biomass without net addition of carbon dioxide to the atmosphere [2–4]. Steam reforming is the main route for the production of hydrogen from ethanol. Noble metals such as Rh, Pt, Pd [5–10], bimetallic oxides such as Ni–Rh catalysts [11,12], and transition metals such as Ni, Co show good catalytic performance for steam reforming of ethanol (SRE) [13,14]. Compared with noble metals, inexpensive Ni- and Co-based catalysts have been studied extensively for SRE. The Ni-based catalysts, such as Ni/Al_2O_3, Ni/MgO, $Ni–Cu/SiO_2$, $Ni–Cu/Al_2O_3$, $NiO–CeO_2–ZrO_2$, Ni/La_2O_3, Ni/Y_2O_3, show good activity and selectivity for SRE, while deactivation resulted from coke formation or carbon deposition is a severe problem as reported in literature [15–20]. The Co-based catalysts, such as Co/Al_2O_3, Co/SiO_2, Co/MgO and $Co/SrTiO_3$ [21–24], are active and more selective than Ni-based catalysts. One of the key disadvantages for Co-based catalysts is also the deactivation caused by coke formation. Among the Co-based catalysts reported, Co/ZnO shows the best catalytic performance [25–27]. However, as indicated by Llorca, Co/ZnO is readily deactivated due to the coke formation or sintering of catalyst particles.

Lots of results on deactivation of Co- and Ni-based catalysts for methane reforming and reaction of F–T have been reported [28–30]. For example, Tsipouriari et al. and Goala et al. studied carbon deposition over Ni/Al_2O_3 catalyst in synthesis gas production from methane reforming [31,32] and Ali et al. suggested that carbon deposited on catalysts surface is one of the main reasons for the deactivation of catalysts for F–T synthesis [33]. However, there are much fewer reports on the deactivation of Co- and Ni-based catalyst for SRE reaction. Zhang studied the catalytic performance of Co, Ni and Ir catalysts supported on CeO_2 for SRE reaction and pointed out that high oxygen storage/release capacity of CeO_2, the interaction between active component and support and the high disperse of the active component would lead to comparably good anti-carbon deposition ability of these catalysts, while in his study, the main subject is not carbon deposition [34].

In our previous papers [35,36], it was reported that Co/CeO_2 exhibited high catalytic activity, selectivity and good stability for SRE. In this work, coke deposition over Co/CeO_2 catalysts was studied.

* Corresponding author.
E-mail addresses: hongwang396@126.com (H. Wang), yuanliu@tju.edu.cn, llwinwill@163.com, leieli_112@yahoo.com.cn (Y. Liu).

1385-8947/$ – see front matter © 2008 Elsevier B.V. All rights reserved.
doi:10.1016/j.cej.2008.02.021

2. Experiment

2.1. Preparation of catalysts

The solution of cobalt nitrate (0.5 mol/l) and the solution of cerium nitrate (0.5 mol/l) were mixed to obtain the solution of cobalt and cerium nitrate. The sodium carbonate solution was used as the precipitator and the mixed solution of cobalt and cerium nitrate was merged into distilled water at a pH of 7.5–8.5 and then stirred for 4 h. The deposit was aged at room temperature for 24 h and then filtrated and was washed with de-ionized water. The deposit was dried at 80 °C for 12 h and calcined at 650 °C for 2 h to obtain Co/CeO_2 catalysts, where the weight fraction of Co_3O_4 in Co/CeO_2 catalyst is 10%.

2.2. Catalytic tests

Catalytic performance tests were carried out in a fixed-bed quartz reactor. About 150 mg catalysts with 40–60 mesh grain size were loaded into the reactor. Prior to each test, the system was flushed with N_2 for 10 min, then reduced in 5 vol.% H_2/Ar at 650 °C for 40 min and then cooled down to reaction temperature.

Reaction mixture consisted of a premixed 20 vol.% water–ethanol solution with 3:1 of molar ratio and 80 vol.% N_2. The space velocity was $40,000\,\mathrm{ml\,g_{cat}^{-1}\,h^{-1}}$, that is about $100{,}000\,\mathrm{h^{-1}}$. The effluent gases were analyzed on-line with SP2100 gas chromatograph. H_2, N_2, CO, CH_4 and CO_2 were separated by TDX-01 column with high pure He as carrier gas. Porapack Q packed column was used to analyze water, acetaldehyde, ethanol and acetone with high pure H_2 as carrier gas. TCD was used as detector.

Conversions and product distributions were calculated using following equations:

$$X_{\mathrm{EtOH}} = \frac{n\mathrm{EtOH}_{\mathrm{in}} - n\mathrm{EtOH}_{\mathrm{out}}}{n\mathrm{EtOH}_{\mathrm{in}}} \times 100\% \quad (1)$$

$$S_i = \frac{nP_i}{\sum_{i=1}^{n} nP_i} \quad (2)$$

where X_{EtOH} is the conversion of ethanol, S_i the distribution of different components in the products, P_i the different components in the reaction products, and n is the amounts of moles.

2.3. Characterization of carbon deposited

The textural tests for carbon deposition were performed using a transmission electron microscope (JEOL JEM-100CX) equipped with energy-dispersive X-ray (EDX) instrument. The TG–DTA experiments were performed on a thermal analysis instrument (DTG-50/50H, Shimadzu Corp.) with a heating rate of 10 °C/min in flowing air. 4.0–6.0 mg catalysts were used for each measurement.

3. Results and discussion

3.1. Variations of ethanol conversion and product distribution with reaction temperature and time

Fig. 1 shows the variation of ethanol conversion with reaction time at several reaction temperatures over Co/CeO_2 catalyst. When reaction temperature is 350 °C, 400 °C or 450 °C, ethanol conversions decrease rapidly with time on stream. When temperature is 500 °C or higher, C_2H_5OH conversions are about 97% and exhibit little change in the 8-h running period.

The variations of product distribution with reaction temperature and time are shown in Fig. 2. As reaction temperature is 500 °C or higher, the traces for variation of product distribution with temperature at different reaction time are nearly the same, so product

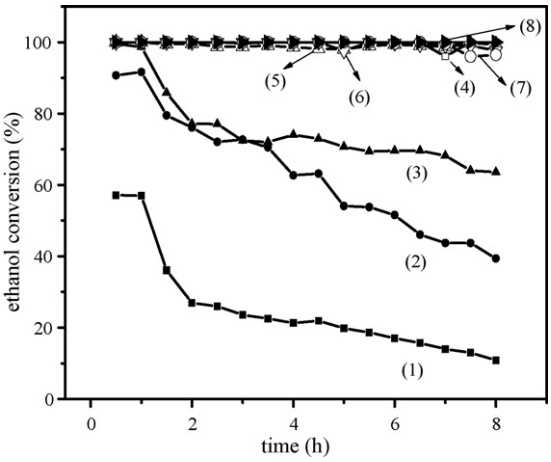

Fig. 1. Variation of C_2H_5OH conversions with reaction time over Co/CeO_2 catalyst at reaction temperatures of (1) 350 °C, (2) 400 °C, (3) 450 °C, (4) 500 °C, (5) 550 °C, (6) 600 °C, (7) 650 °C and (8) 700 °C.

distribution at reaction temperatures of higher than 500 °C is given only in Fig. 2a (reacted for 2 h). In the reaction temperature range of 500–700 °C, the fraction of H_2 in product gases is close to 65%, the fraction of CH_4 is under 4% and C_2-products are close to zero. The content of CO increases while that of CO_2 decreases with the increase of reaction temperature, which should be partly due to reverse water gas shift reaction which converts CO_2 to CO.

As reaction temperatures were 350 °C, 400 °C and 450 °C, the contents of CH_3CHO, CH_3COCH_3 and/or C_2H_4 in reacted products are at a high level, indicating that dehydrogenation and dehydration of ethanol prevail at these reaction temperatures. The variation of the product distribution with reaction time at the same reaction temperatures can be seen by comparing Fig. 2a–d (corresponding to reaction time of 2 h, 4 h, 6 h and 8 h) at the specific reaction temperatures. As the reaction time increases, the content of C_2H_4 increases, suggesting that the rate of dehydration increase, which is likely be due to that some of the active sites for dehydrogenation are deactivated by deposited carbon thus leading to more ethanol being dehydrated to C_2H_4. The content of CH_3CHO presented a peak at reaction temperature of 450 °C, showing that dehydrogenation rate at this temperature is high while the following reaction's rate is slower.

It is generally accepted that reaction network for SRE is composed of two parallel reaction route, as shown in Fig. 3 [5,13,15,37–41]. The one route is dehydrogenation of ethanol to produce CH_3CHO, then CH_3CHO is decomposed and then the steam reforming of CH_4, and so on. The other is dehydration of ethanol to form C_2H_4 and then the cleavage of C—C bond or formation of coke, and so on. Although detailed mechanism cannot be given, the results of product distribution shown in Fig. 2 suggest that the SRE over this Co/CeO_2 catalyst is carried out through the two parallel reaction ways similar to that of listed in Fig. 3. There is no CH_3COCH_3 in Fig. 3, while CH_3COCH_3 was detected obviously over Co/CeO_2 catalysts in this work. Nishiguchi et al. [42] have studied the formation mechanism of CH_3COCH_3 in SRE and suggested that CH_3COCH_3 is produced from CH_3CHO. In Fig. 3, SR and WG stand for steam reforming and water gas shift reaction, respectively.

3.2. TG–DTA

Fig. 4 shows the DTA and TG results of used Co/CeO_2 catalysts. The exothermic peaks in DTA curves should be attributed to the combustion of coke deposited and the peaks at different tempera-

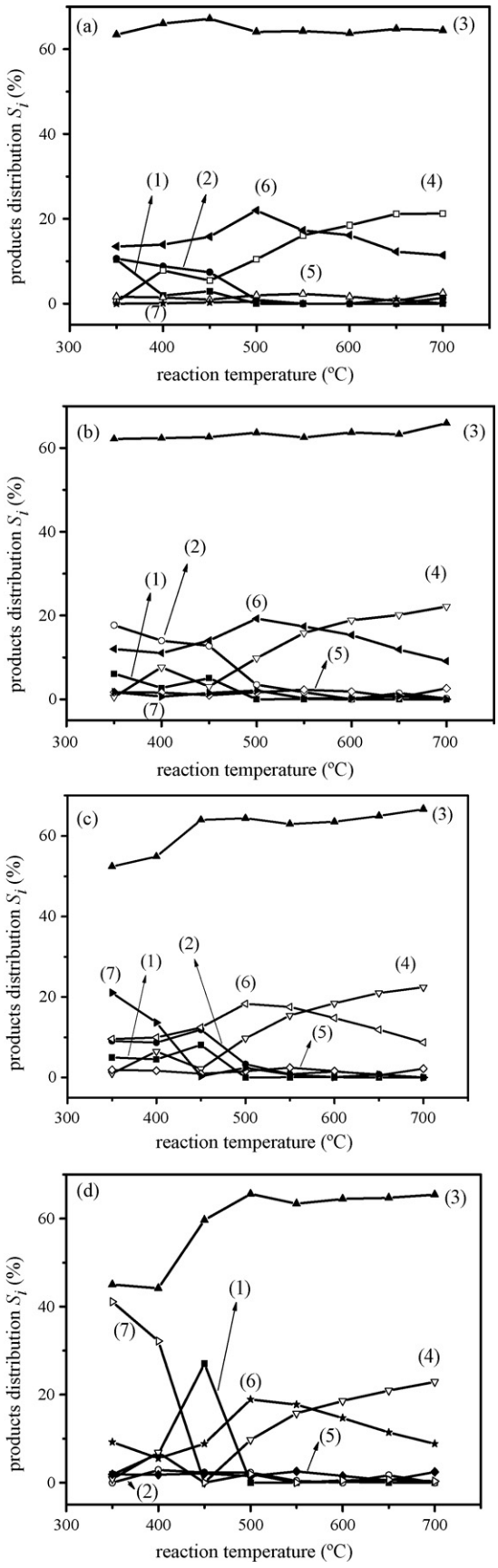

Fig. 2. Variation of product distribution with reaction temperature over Co/CeO_2 catalyst reacted for: (a) 2 h, (b) 4 h, (c) 6 h and (d) 8 h. (1) CH_3CHO, (2) CH_3COCH_3, (3) H_2, (4) CO, (5) CH_4, (6) CO_2, and (7) C_2H_4.

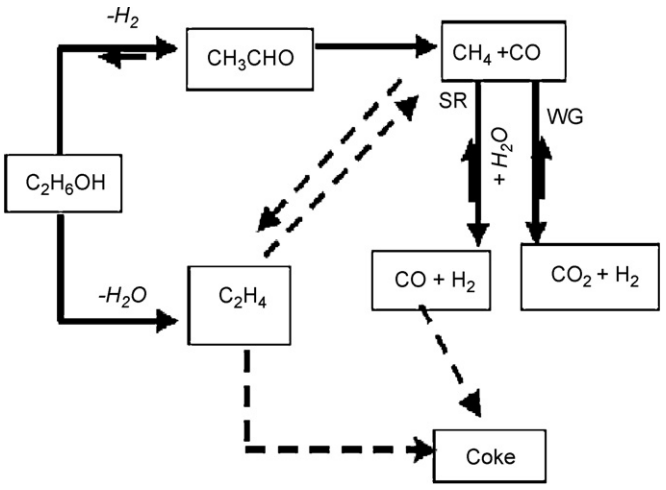

Fig. 3. Sketch map of reaction pathway for catalytic steam reforming of ethanol [5,13,15,37–41].

ture relate with different properties of the coke.

The detected products of reaction were comprised of CO, CO_2, CH_4, C_2H_4, CH_3CHO, CH_3COCH_3 and H_2, thus the possible coke formation ways are listed as following and reactions of steam reforming of ethanol (8) and (9) are also listed here [43,44]:

$$CH_4 \rightarrow C + 2H_2 \quad (3)$$

$$2CO \rightarrow C + CO_2 \quad (4)$$

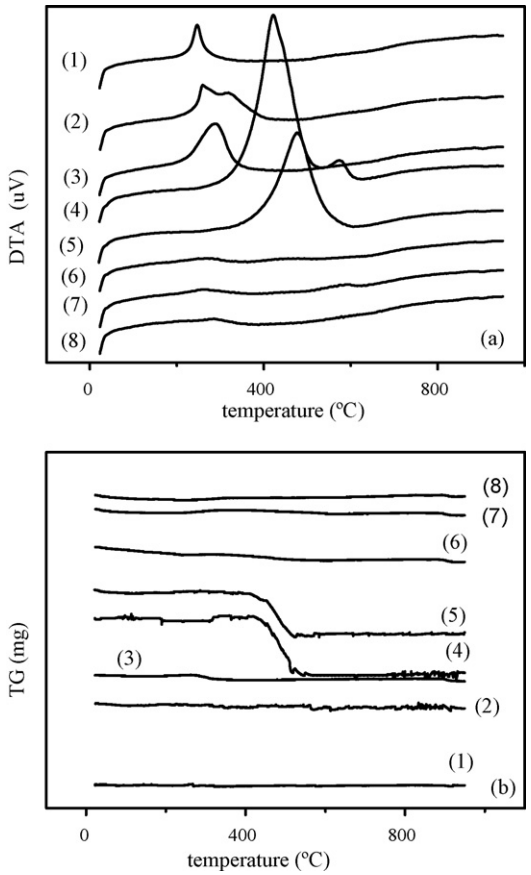

Fig. 4. DTA–TG results of Co/CeO_2 catalysts reacted at temperatures of: (1) 350 °C, (2) 400 °C, (3) 450 °C, (4) 500 °C, (5) 550 °C, (6) 600 °C, (7) 650 °C and (8) 700 °C for 8 h. (a) DTA curves and (b) TG curves.

$$C_2H_5OH \rightarrow C_2H_4 + H_2O, \quad C_2H_4 \rightarrow \text{polymers} \rightarrow \text{coke} \tag{5}$$

$$C_2H_5OH \rightarrow CH_3CHO + H_2, \quad CH_3CHO \rightarrow CH_3COCH_3 \rightarrow \text{coke} \tag{6}$$

$$CH_3CHO \rightarrow \text{coke} \tag{7}$$

$$C_2H_5OH + 3H_2O \rightarrow 6H_2 + 2CO_2 \tag{8}$$

$$C_2H_5OH + H_2O \rightarrow 4H_2 + 2CO \tag{9}$$

In order to make out the coke deposited at 350 °C, 400 °C and 450 °C, the reaction scheme at these temperatures should be analyzed in advance. As can be seen from the corresponding product distribution shown in Fig. 2d (data of 350 °C), the reacted products over this catalyst at 350 °C for 8 h contain 45% H_2, 41% C_2H_4 and 9% CO_2. If the H_2 was produced through SRE of (8), the content of H_2 should be less than 27%, which is three times of the content of CO_2 as dictated by Eq. (8). The CO content in the products at 350 °C is lower than 2%, so H_2 is not formed mainly through reaction (9). On the other hand, SRE is a serial reaction as shown in Fig. 3, and it was reported that dehydrogenation could be generated facilely at cobalt sites [36]. It is seen from Fig. 2 that the H_2 content in the reacted gas mixtures rises concomitant with that of CH_3CHO. This result indicates that dehydrogenation of ethanol is a main reaction and the dehydrogenation contributes a large part of H_2 produced.

The variation of product distribution with reaction time can be observed by comparing data in Fig. 2a–d at 350 °C, 400 °C and 450 °C. As the reaction time increases, the content of CH_3CHO and CH_3COCH_3 decreases and the content of ethene increases. Coke should be formed through reactions (6) and (7), and the amount of coke deposited increases with time on stream and thus active sites for ethanol dehydrogenation are covered by the coke gradually, leading to the decrease of CH_3CHO and CH_3COCH_3 formation.

As reaction time increases, the amount of C_2H_4 produced increases markedly, especially as reacted for 8 h (Fig. 2d), the content of C_2H_4 in reacted gas mixtures is much high. So it could be speculated that as the active sites for dehydrogenation of ethanol be deactivated gradually, the dehydration of ethanol would prevail.

Based on the above analysis, the coke formation in reaction temperature range of 350–450 °C is proposed here. As the reaction time is comparatively short, ethanol is dehydrogenated to produce CH_3CHO and hydrogen and then the CH_3CHO is converted to CH_3COCH_3 and other products. At this period, coke mainly comes from reactions (6) and (7). As the reaction time increases, the active sites for dehydrogenation are covered by the coke, deposited step by step, and more ethanol is dehydrated to produce ethene, so the amount of coke formed through reaction (5) increases.

In Fig. 4, the exothermic peaks attributed to coke combustion shift to higher temperature with reaction temperature increase, indicating the nature of the coke deposited may not be the same at different reaction temperature.

When the reaction temperature is over 500 °C, the reacted products consist of H_2, CO, CO_2 and miner CH_4, indicating the main reaction is steam reforming of ethanol. As shown in TEM diagram (will discuss in Section 3.3), tube- or fiber-like carbons were formed at these temperatures. It is supposed that carbon deposition at these temperatures comes from reactions (3)–(7). Although CH_3CHO, C_2H_4 and CH_3COCH_3 could not be detected over 500 °C, the nature of the active sites of the catalyst should be the same as it is reacted under 450 °C, so the reaction of dehydrogenation and dehydration still was on going over 500 °C. Hence the coke was still in forming through reactions of (5)–(7), while the coke deposited is transformed to tube- or fiber-like carbons at these temperatures.

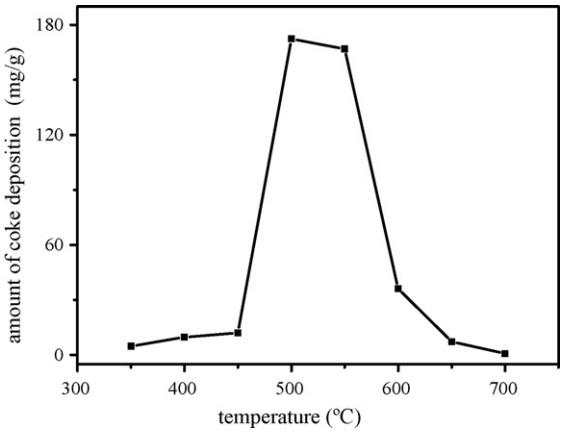

Fig. 5. Variation of amount of coke deposition with reaction temperature over Co/CeO_2 catalyst reacted for 8 h.

Separate experimental results in our lab show that disproportionation of CO and cracking of CH_4 start to happen over Co/CeO_2 catalysts at 500 °C. No studies on disproportionation of CO and cracking of CH_4 over Co/CeO_2 catalysts are found in literatures, while the two reactions catalyzed by metal cobalt with other supports have been reported. Pinheiro et al. have studied carbon deposition from CO disproportionation over Co/MgO catalysts and pointed out that carbon nanotubes are obtained from $CO + H_2$ mixtures in the 500–600 °C range [45]. In another paper, they found that the CO disproportionation reaction over Co/Al_2O_3 catalysts leads to the formation of carbon nanotubes in the 500–600 °C range [46]. Metal cobalt can catalyze methane cracking to produce carbon microfibers and hydrogen too [47]. So it is proposed that part of the carbon deposition comes from reactions (3) and (4) at reaction temperatures of 500 °C and 550 °C in the SRE process of this work.

When reaction temperature is over 600 °C, the reaction rate for steam and CO_2 reforming of carbon deposition is high enough to eliminate the carbon deposited on catalyst surface, so the carbon deposition is hard to be observed.

The specific weights of coke or carbon deposited on catalyst surface can be obtained from TG results (Fig. 4b), which are shown in Fig. 5. The amount of carbon deposited on catalysts reacted at 500 °C and 550 °C is much higher than that of any other reaction temperatures. The amount of carbon deposited is 172.36 mg/g at reaction temperature of 500 °C, while the amount is 0.82 mg/g at 700 °C. In correlation with catalytic reactivity shown in Fig. 1, ethanol conversions decrease markedly with the reaction times at 450 °C, 400 °C and 350 °C, although the coke formed is few at these temperatures, while no apparent decreases of ethanol conversions with the reaction time can be observed as the reaction temperature is 500 °C or 550 °C, and at these temperatures the amount of carbon deposited is much higher. This result indicates that the cokes formed through reactions (5)–(7) at temperatures under 450 °C lower catalytic activity severely. Comparatively, at reaction temperature of 500 °C or 550 °C, the coke is transformed to fiber- or tube-like carbons (see TEM results) and the deactivation caused by carbon deposited is insignificant.

3.3. TEM

Fig. 6 shows TEM images of catalysts reacted at different temperatures for 8 h.

The catalysts reacted at 350 °C and 450 °C for 8 h exhibit the similar textural feature (Fig. 6a and b), and a typical catalyst particle with more magnified picture is shown beside the Fig. 6b. It is seen from the magnified picture that the catalyst particle is enclosed

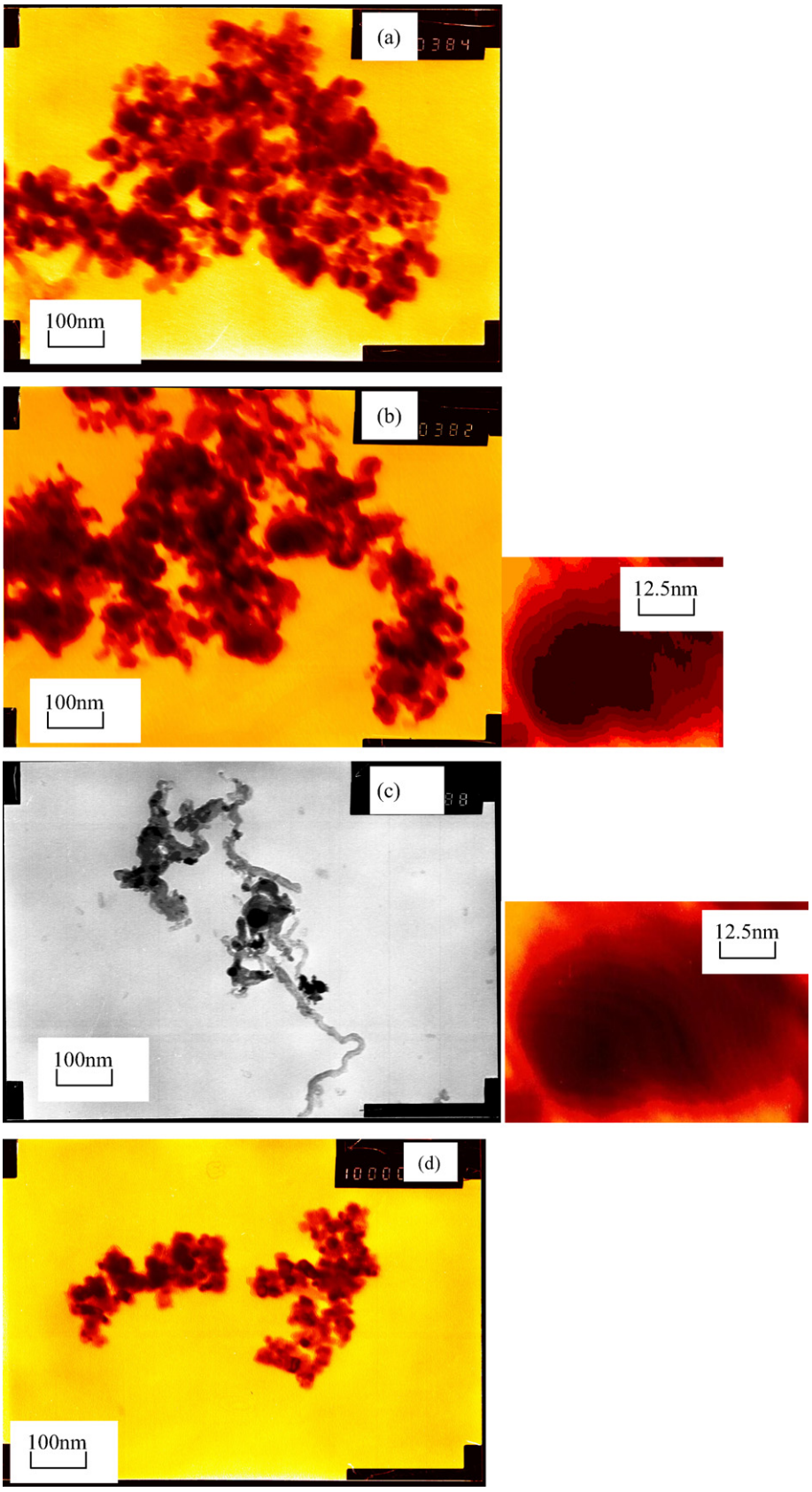

Fig. 6. TEM images of Co/CeO_2 catalysts reacted for 8 h at: (a) 350 °C, (b) 450 °C, (c) 500 °C, and (d) 700 °C.

by layer, and EDX analysis reveals that the layers are mainly composed of carbon. That is, the catalyst particles are enclosed by the coke, which is formed through the reactions of (5)–(7) when reaction temperature is at 350 °C and 450 °C. The coke formation and encapsulation of catalyst particles result in the severe deactivation of the catalysts.

As reaction temperature is 500 °C, fiber- or tube-like carbons are formed (Fig. 6c) and the fiber- or tube-like carbons stretch away from the catalyst particles, thus the encapsulation of catalyst particles is much lighter. From the magnified picture of a typical catalyst particle beside Fig. 6c, it can be seen that no layered coke exists. This is the reason why no apparent deactivation was observed at reaction temperatures of 500 °C and 550 °C although large amount of carbon was deposited, while severe deactivation was observed with much fewer cokes formed at 450 °C and below.

When the reaction temperature is 700 °C, the coke formation or carbon deposition is hardly seen (Fig. 6d), neither layered coke nor fiber- or tube-like carbons be observed.

According to the DTA–TG and TEM results, the carbon deposition at the temperatures of 600 °C and 700 °C is rarely observed, suggesting that carbon deposition is not a main problem on Co/CeO_2 catalysts for SRE at the high reaction temperatures.

4. Conclusion

The process of coke formation or carbon deposition over Co/CeO_2 catalysts for steam reforming of ethanol depends on reaction temperature. When the reaction temperature is 450 °C and lower, ethanol is dehydrogenated and/or dehydrated over Co/CeO_2 catalysts and the dehydrogenated and dehydrated products are further transformed to cokes. When the reaction temperature is 500 °C or 550 °C, disproportionation reaction of CO and cracking of CH_4 also contributes part of carbon deposition. In the former case, catalyst particles were enclosed by the coke, leading to severe deactivation, while in the latter case the encapsulation of catalyst particles by carbon deposited was insignificant due to that the coke is transformed to fiber- or tube-like carbons which stretches away from catalyst particles, and thus the deactivation was not observed. When the reaction temperature is 600 °C or higher, carbon deposition is not a main problem for steam reforming of ethanol over Co/CeO_2 catalysts, for carbon deposition or coke formation at these temperatures is slight.

Acknowledgments

The financial support of this work by Hi-tech Research and Development Program of China (863 program, granted as No. 2006AA05Z115 and 2007AA05Z104) and by the Cheung Kong Scholar Program for Innovative Teams of the Ministry of Education (No. IRT0641) is gratefully acknowledged. The authors also thank Dr. Q.H. Yang for helpful discussions.

References

[1] Y. Tanaka, T. Utaka, R. Kikuchi, K. Sasaki, K. Eguchi, Water gas shift reaction over Cu-based mixed oxides for CO removal from the reformed fuels, Appl. Catal. A 242 (2003) 287–295.
[2] M. Momirlan, T. Veziroglu, Recent directions of world hydrogen production renewable and sustainable energy, Reviews 3 (1999) 219–231.
[3] D. Das, T.N. Veziroglu, Hydrogen production by biological processes: a survey of literature, Int. J. Hydrogen Energy 26 (2001) 13–28.
[4] A.N. Fatsikostas, D.I. Kondarides, X.E. Verykios, Production of hydrogen for fuel cells by reformation of biomass-derived ethanol, Catal. Today 75 (2002) 145–155.
[5] J.P. Breen, R. Burch, H.M. Coleman, Metal-catalysed steam reforming of ethanol in the production of hydrogen for fuel cell applications, Appl. Catal. B 39 (2002) 65–74.
[6] S. Cavallaro, V. Chiodo, V. Vita, S. Freni, Hydrogen production by auto-thermal reforming of ethanol on Rh/Al_2O_3 catalyst, J. Power Sources 123 (2003) 10–16.
[7] C. Diagne, H. Idriss, A. Kiennemann, Hydrogen production by ethanol reforming over $Rh/CeO_2–ZrO_2$ catalysts, Catal. Commun. 3 (2002) 565–571.
[8] R.M. Navarro, M.C.Á. lvarez-Galván, M.C. Sánchez-Sánchez, F. Rosa, J.L.G. Fierro, Production of hydrogen by oxidative reforming of ethanol over Pt catalysts supported on Al_2O_3 modified with Ce and La, Appl. Catal. B 55 (2005) 229–241.
[9] D.K. Liguras, D.I. Kondarides, X.E. Verykios, Production of hydrogen for fuel cells by steam reforming of ethanol over supported noble metal catalysts, Appl. Catal. B 43 (2003) 345–354.
[10] S. Cavallaro, V. Chiodo, S. Freni, N. Mondello, F. Frusteri, Performance of Rh/Al_2O_3 catalyst in the steam reforming of ethanol: H_2 production for MCFC, Appl. Catal. A 249 (2003) 119–128.
[11] J. Kugai, S. Velu, C.S. Song, M.H. Engelhard, Y.H. Chin, Effects of nanocrystalline CeO_2 supports on the properties and performance of Ni–Rh bimetallic catalyst for oxidative steam reforming of ethanol, J. Catal. 238 (2006) 430–440.
[12] J. Kugai, S. Velu, C.S. Song, Low-temperature reforming of ethanol over CeO_2-supported Ni–Rh bimetallic catalysts for hydrogen production, Catal. Lett. 101 (2005) 255–264.
[13] A. Therdthianwong, T. Sakulkoakiet, S. Therdthianwong, Hydrogen production by catalytic ethanol steam reforming, Science Asia 27 (2001) 193–198.
[14] N.A. Fatsikostas, X.E. Verykios, Reaction network of steam reforming of ethanol over Ni-based catalysts, J. Catal. 225 (2004) 439–452.
[15] J. Comas, F. Mariño, M. Laborde, N. Amadeo, Bio-ethanol steam reforming on Ni/Al_2O_3 catalyst, Chem. Eng. J. 98 (2004) 61–68.
[16] S. Freni, S. Cavallaro, N. Mondello, et al., Steam reforming of ethanol on Ni/MgO catalysts: H_2 production for MCFC, J. Power Sources 108 (2002) 53–57.
[17] J. Sun, F. Wu, X.P. Qiu, et al., Hydrogen production from ethanol steam reforming over Ni/Al_2O_3 and Ni/La_2O_3 catalysts at low temperature, Chin. J. Catal. 25 (2004) 551–555.
[18] J. Sun, X.P. Qiu, F. Wu, et al., H_2 from steam reforming of ethanol at low temperature over Ni/Y_2O_3, Ni/La_2O_3 and Ni/Al_2O_3 catalysts for fuel-cell application, Int. J. Hydrogen Energy 30 (2005) 437–445.
[19] F. Frusteri, S. Freni, V. Chiodo, et al., Potassium improved stability of Ni/MgO in the steam reforming of ethanol for the production of hydrogen for MCFC, J. Power Sources 132 (2004) 139–144.
[20] D. Srinivas, C.V.V. Satyanarayana, H.S. Potdar, et al., Structural studies on $NiO–CeO_2–ZrO_2$ catalysts for steam reforming of ethanol, Appl. Catal. A 246 (2003) 323–334.
[21] M.S. Batista, R.K.S. Santos, E.M. Assaf, J.M. Assaf, E.A. Ticianelli, Characterization of the activity and stability of supported cobalt catalysts for the steam reforming of ethanol, J. Power Sources 124 (2003) 99–103.
[22] K. Urasaki, K. Tokunaga, Y. Sekine, E. Kikuchi, M. Matsukata, Hydrogen production by steam reforming of ethanol using cobalt and nickel catalysts supported on strontium titanate, Chem. Lett. 34 (2005) 668–669.
[23] M.S. Batista, R.K.S. Santos, E.M. Assaf, J.M. Assaf, E.A. Ticianelli, High efficiency steam reforming of ethanol by cobalt-based catalysts, J. Power Sources 134 (2004) 27–32.
[24] D.R. Sahoo, S. Vajpai, S. Patel, K.K. Pant, Kinetic modeling of steam reforming of ethanol for the production of hydrogen over Co/Al_2O_3 catalyst, Chem. Eng. J. 125 (2007) 139–147.
[25] J. Llorca, N. Homs, P.R. Piscina, In situ DRIFT-mass spectrometry study of the ethanol steam-reforming reaction over carbonyl-derived Co/ZnO catalysts, J. Catal. 227 (2004) 556–560.
[26] J. Llorca, N. Homs, J. Sales, J.G. Fierro, P.R. Piscina, Effect of sodium addition on the performance of Co–ZnO-based catalysts for hydrogen production from bioethanol, J. Catal. 222 (2004) 470–480.
[27] J. Llorca, N. Homs, J. Sales, P.R. Piscina, Efficient production of hydrogen over supported cobalt catalysts from ethanol steam reforming, J. Catal. 209 (2002) 306–317.
[28] J.R. Rostrup-Nielsen, Production of synthesis gas, Catal. Today 18 (1993) 305–324.
[29] S.C. Tsang, J.B. Claridge, M.L.H. Green, Recent advances in the conversion of methane to synthesis gas, Catal. Today 23 (1995) 3–15.
[30] F. Rohr, O.A. Lindvåg, A. Holmen, E.A. Blekkan, Fischer–Tropsch synthesis over cobalt catalysts supported on zirconia-modified alumina, Catal. Today 58 (2000) 247–254.
[31] V.A. Tsipouriari, A.M. Ettathiou, Z.L. Zhang, et al., Reforming of methane with carbon dioxide to synthesis gas over supported Rh catalysts, Catal. Today 21 (1994) 579–587.
[32] M.A. Goala, A.A. Lemonidou, A.M. Ettathiou, Characterization of carbonaceous species formed during reforming of CH_4 with CO_2 over $Ni/CaO–Al_2O_3$ catalysts studied by various transient techniques, J. Catal. 161 (1996) 626–640.
[33] S. Ali, B. Chen, J.G. Goodwin, Zr promotion of Co/SiO_2 for Fischer–Tropsch synthesis, J. Catal. 157 (1995) 35–41.
[34] B.C. Zhang, X.L. Tang, Y. Li, et al., Steam reforming of bio-ethanol for the production of hydrogen over ceria supported Co, Ir and Ni catalysts, Catal. Commun. 7 (2006) 367–372.
[35] H. Wang, P.X. Liu, Y. Liu, Y.N. Qin, Study on Co/CeO_2 catalysts for ethanol steam reforming, Chin. J. Catal. 27 (2006) 977–982.
[36] H. Wang, J.L. Ye, Y. Liu, Y.D. Li, Y.N. Qin, Steam reforming of ethanol over Co_3O_4/CeO_2 catalysts prepared by different method, Catal. Today 129 (2007) 305–312.

[37] P.Y. Sheng, H. Idriss, Ethanol reactions over Au–Rh/CeO_2 catalysts, total decomposition and H_2 formation, JVST A 22 (4) (2004) 1652–1658.
[38] S. Zhao, T. Luo, R.J. Gorte, Deactivation of the water-gas-shift activity of Pd/Ceria by Mo, J. Catal. 221 (2004) 413–420.
[39] A. Yee, J. Morrisons, H. Idriss, A study of the reactions of ethanol on CeO_2 and Pd/CeO_2 by steady state reactions, temperature programmed desorption, and in situ FT-IR, J. Catal. 186 (1999) 279–295.
[40] A. Yee, J. Morrisons, H. Idriss, A study of ethanol reactions over Pt/CeO_2 by temperature-programmed desorption and in situ FT-IR spectroscopy: evidence of benzene formation, J. Catal. 191 (2000) 30–45.
[41] A. Yee, J. Morrisons, H. Idriss, The reactions of ethanol over M/CeO_2 catalysts: evidence of carbon–carbon bond dissociation at low temperatures over Rh/CeO_2, Catal. Today 63 (2000) 327–335.
[42] T. Nishiguchi, T. Matsumoto, K. Kanai, et al., Catalytic steam reforming of ethanol to produce hydrogen and acetone, Appl. Catal. A 279 (2005) 273–277.
[43] P. Biswas, D. Kunzru, Oxidative steam reforming of ethanol over Ni/CeO_2–ZrO_2 catalyst, Chem. Eng. J. 136 (2008) 41–49.
[44] P.D. Vaidya, A.E. Rodrigues, Insight into steam reforming of ethanol to produce hydrogen for fuel cells, Chem. Eng. J. 117 (2006) 39–49.
[45] J.P. Pinheiro, M.C. Schouler, P. Gadelle, Nanotubes and nanofilaments from carbon monoxide disproportionation over Co/MgO catalysts. I. Growth versus catalyst state, Carbon 41 (2003) 2949–2959.
[46] J.P. Pinheiro, M.C. Schouler, E. Dooryhee, In situ X-ray diffraction study of carbon nanotubes and filaments during their formation over Co/Al_2O_3 catalysts, Solid State Commun. 123 (3–4) (2002) 161–166.
[47] L.Z. Gao, S. Kawi, The production of straight carbon microfibers by the cracking of methane over Co-SBA-15 catalysts, Catal. Lett. 118 (3–4) (2007) 211–218.